

Ventilator-induced Cell Wounding and Repair in the Intact Lung

Ognjen Gajic, Jaeho Lee, Clinton H. Doerr, Jorge C. Berrios, Jeffrey L. Myers, and Rolf D. Hubmayr

Department of Medicine, Division of Pulmonary and Critical Care Medicine, Thoracic Diseases Research Unit; Department of Pathology; and Department of Physiology and Biophysics, Mayo Clinic, Rochester, Minnesota

We tested the hypothesis that cells of ventilator-injured lungs are subject to reversible plasma membrane stress failure. Rat lungs were perfused with the membrane impermeable fluorescent marker propidium iodide and randomized to one of four ventilation strategies. Subpleural lung regions were imaged with confocal microscopy, and cell injury was quantified as the number of propidium iodide-positive cells per alveolus. The number of injured cells was significantly greater in lungs ventilated with large tidal volumes and zero end-expiratory pressure than in lungs ventilated with small tidal volumes and positive end-expiratory pressure ($p < 0.01$). Cell injury correlated with lung weight gain, change in dynamic compliance, and histologic injury scores. In a second set of experiments, lungs were mechanically ventilated for 30 minutes at high tidal volume settings, whereas propidium iodide was perfused either during or after injurious ventilation. Labeling after removal of injurious stress revealed significantly fewer injured cells (0.25 ± 0.09 to 0.08 ± 0.08 , $p < 0.01$). We conclude that cells of ventilator-injured lungs are subject to reversible plasma membrane stress failure.

Keywords: ventilator-induced lung injury; plasma membrane resealing; confocal microscopy; isolated perfused rat lung; stress failure

Ventilator-induced lung injury (VILI) is characterized by mechanical failure of the blood-gas barrier. As shown with electron microscopy more than 20 years ago, widespread endothelial and epithelial cell injury is one of the hallmarks of the entity and accounts at least in part for the increased microvascular permeability of ventilator-injured lungs (1–5). Plasma membrane blebs and cytoskeletal disruptions occur in association with intercellular and intracellular gaps exposing basement membrane. Whereas electron microscopy defines cellular ultrastructure in intricate detail, the technique is limited by finite sampling and is therefore not well suited for quantifying injury on the scale of whole lungs. Light microscopy, on the other hand, does not have sufficient spatial resolution to define lesions in individual cells. Therefore, much VILI research has focused on the consequences of cellular injury such as edema, inflammation, and tissue remodeling rather than on the determinants of the cellular stress failure itself (6–8).

We introduce a new method for grading mechanical lung injury that rests on the assessment of cell membrane integrity and that involves confocal imaging of subpleural lung regions. The lung is perfused with the membrane impermeable label

propidium iodide (PI) (Molecular Probe, Eugene, OR). When PI enters a cell through a membrane defect, it intercalates with DNA and emits a red fluorescence upon excitation with blue light. We have previously reported on the use of PI as a marker of plasma membrane stress failure in cultured alveolar epithelial cells and have now adapted this method for the study of mechanically ventilated isolated perfused lungs (9, 10).

Plasma membrane stress failure occurs when the matrix to which a cell adheres undergoes large deformations (1, 11–14). As a result, the cell might be forced to assume a shape with a large surface-to-volume ratio at which the plasma membrane might experience lytic tension. Most breaks are repaired within seconds, usually via a calcium-dependent lipid trafficking response (15–17). Failure to reseal the membrane defect invariably leads to cell death. The ultimate fate of wounded and resealed lung cells is unclear. In many instances, wounded and resealed cells maintain normal function. In certain model systems, wounding causes expression of early response genes associated with the translocation of the nuclear transcription factor nuclear factor- κ B (18). This raises the important question whether the proinflammatory state associated with large volume mechanical ventilation is the result of transient cell injury (18) or the consequence of cellular mechanotransduction (19–22).

The primary objective of the experiments described in this report was to test the hypothesis that cells of ventilator-injured lungs are subject to plasma membrane stress failure. To this end, we compared a PI uptake-based index of cell wounding with conventional injury markers such as weight gain, change in lung compliance, change in pulmonary vascular resistance, and light microscopy. Our secondary objective was to assess the potential for cell resealing under conditions of injurious stress. We compared the cell injury index of lungs that were PI perfused during high-volume ventilation with that of lungs that were PI perfused after high-volume ventilation. The latter had consistently fewer PI-positive cells. This finding suggests that most wounded cells reseal their membrane defect and that a relatively small fraction of wounded lung cells undergo necrosis.

METHODS

Animal Preparation

Male adult Sprague-Dawley rats weighing 275 to 380 g were anesthetized by intraperitoneal administration of sodium pentobarbital (50 mg/kg). A tracheostomy was performed, and the lungs were mechanically ventilated with a tidal volume (VT) of 6 ml/kg (Harvard Rodent Ventilator, Model 683; South Natick, MA). The thorax was opened, and heparin was administered into the right ventricle. The animal was killed by exsanguination. The pulmonary artery and the left atrium were cannulated and perfused with a red cell-enriched 4% dextran (40KD) in Krebs bicarbonate buffer (37°C) at a flow rate of 6 ml/minute. Fluorescent label PI was added to the perfusate either during or after experimental ventilation. Ventilator stroke volume, inspiratory CO₂ concentration, and airway and vascular pressures were recorded, and the ventilator setting was adjusted according to the experimental protocol. All monitored

(Received in original form August 19, 2002; accepted in final form December 9, 2002)

Supported by a grant from the National Institutes of Health (HL-63178)

Correspondence and requests for reprints should be addressed to Correspondence and requests for reprints should be addressed to Ognjen Gajic, Stabile 8-62, Mayo Clinic, 200 First Street SW, Rochester, MN 55905. E-mail: gajic.ognjen@mayo.edu

This article has an online supplement, which is accessible from this issue's table of contents online at www.atsjournals.org.

Am J Respir Crit Care Med Vol 167, pp 1057–1063, 2003

Originally Published in Press as DOI: 10.1164/rccm.200208-889OC on December 12, 2002

Internet address: www.atsjournals.org

variables were displayed and recorded in digital form with an IBM-PC running in-house-developed, customized software (Labview for Windows; National Instruments Corp., Austin, TX). At the end of the experiment, the lungs and heart were excised en block, weighed, and then submerged in saline for immediate confocal microscopy.

Experimental Protocol

Twenty-five lungs were mechanically ventilated for 30 minutes at a rate of 40 per minute while being perfused with a solution containing 4 $\mu\text{g/ml}$ PI. The lungs were randomized to one of four ventilator management strategies: VT of 6 ml/kg at a positive end-expiratory pressure (PEEP) of 3 cm H₂O (group I); VT of 30 ml/kg at a PEEP of 3 cm H₂O (group II); VT of 40 ml/kg at a PEEP 3 cm H₂O (group III); and VT of 40 ml/kg at a PEEP of 0 cm H₂O (group IV). An additional 17 lungs were mechanically ventilated for 30 minutes at group IV settings. In seven instances, PI was added to the perfusate during the last 5 minutes of injurious mechanical ventilation. In 10 preparations, the label was added only after VT and PEEP settings had been adjusted to noninjurious settings.

Laser Confocal Microscopy-based Assessment of Cell Injury and Resealing in Intact Lungs

The subpleural lung tissue was imaged using an Olympus BH2 confocal microscope (Olympus, Melville, NY) at a depth of up to 50 μm . The specimen was excited with blue laser light, and emission wavelengths were collected on two channels: autofluorescence ($\lambda < 570 \text{ nm}$) on channel 1 and PI ($\lambda > 590 \text{ nm}$) on channel 2. Images were digitized at an eight-bit resolution and were stored in arrays of 512 \times 512 pixels.

In Vitro Validation of a Method to Characterize Cell Injury and Resealing

A549 cells were grown to confluence in Lab-Tek II eight-chambered slides (Nalge Nunc International, Naperville, IL). After adding fluorescent dextran (FDx 70 kD; Sigma, St. Louis, MO) (series 1), PI (series 2), or placebo (series 3) to the media, the slides were placed into an incubator. O₂ and CO₂ tension were adjusted to 200 and 40 mm Hg, respectively, and the monolayers scratched with a surgical blade (Becton Dickinson, Franklin Lakes, NJ). Two minutes later, the slides were washed with 4°C phosphate-buffered saline, were incubated for 2 minutes with PI containing media, and were washed again. Epifluorescence images were obtained at emission peaks of 510 and 620 nm using an inverted microscope (Zeiss, Thornwood, NY). The number of FDx- and PI-positive cells per 20 \times viewfield were counted. Consistent with previous studies on the topic, FDx+ cells of series 1 represent injured cells that have trapped FDx after plasma membrane repair (10, 11, 23, 24). In contrast, PI-positive cells of series 1 and 3 have failed to reseal the membrane defect and are presumably destined to undergo necrosis. The *in vitro* experiments of series 2 (injury in the presence of PI) and 3 (PI added some time later) mimic the labeling sequence used in our whole-lung experiments. PI-positive cells of series 2 represent the total number of injured cells, whereas those of series 3 represent necrotic and nonresealed cells only.

Light Microscopy

The lungs were fixed by intratracheal installation of 10% formalin (15 ml/kg) and were floated in the solution overnight. Subsequently, six random coronal sections (three from each lung, six per experiment) were processed into 5- μm slices and stained with hematoxylin and eosin. The slides were then reviewed by a pathologist who was blinded to the experimental protocol using modified semiquantitative scoring based on the amount of hyaline membranes, perivascular hemorrhage, and small airway epithelial injury (25–26).

Data Analysis

The degree of cell membrane injury was evaluated in a blinded fashion and expressed as a ratio of the number of injured (PI-positive) cells per total number of alveoli in the field from 10 random subpleural images. The presence and degree of cell membrane injury were compared with the change in the dynamic compliance, the amount of lung edema (lung weight gain), and the histology score.

Interobserver variability was evaluated in preliminary experiments

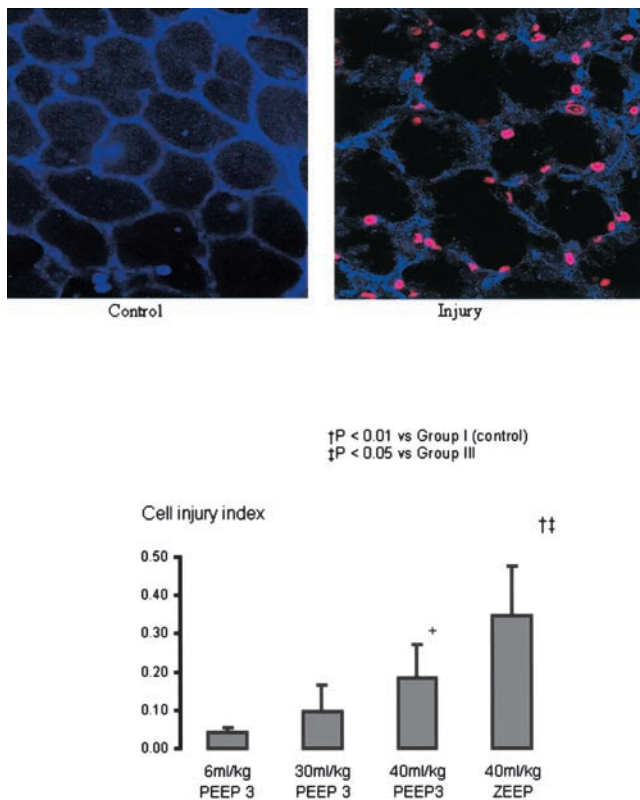


Figure 1. (Top) Confocal images of subpleural alveoli (left, control; right, injury). The red nuclei mark the injured cells (propidium iodide (PI)-positive nuclei). (Bottom) Average number of PI-positive cells per alveolus as assessed from 10 random subpleural fields. PEEP = positive end-expiratory pressure; ZEEP = zero end-expiratory pressure.

by paired comparisons of two blinded raters using Wilcoxon signed-rank test. Analysis of variance and Kruskal-Wallis test were used to test for differences between the groups, followed by Tukey-Kramer test for multiple comparisons (JMP Version 4.04; SAS Institute, Cary, NC).

RESULTS

High-volume Ventilation Is Associated with Plasma Membrane Wounds

High tidal volume ventilation (groups II, III, and IV) caused cellular injury, as evidenced by the presence of PI-positive cells on the fluorescent images (Figure 1, top). The number of PI-positive cells per alveolus (cell injury index) increased from 0.04 \pm 0.01 in group I to 0.10 \pm 0.07 in group II, 0.18 \pm 0.09 in group III, and 0.35 \pm 0.13 in group IV ($p < 0.01$ analysis of variance; Figure 1, bottom). Although groups III and IV were ventilated with the same tidal volume (40 ml/kg), the application of 3 cm H₂O PEEP in group III was associated with a lower number of wounded cells ($p = 0.05$).

There was excellent interobserver agreement with regard to the number of PI-positive cells per alveolus (median interobserver difference in cell injury index in any one experiment = 0.001, range from -0.11 to 0.04, $p = 0.79$). However, there was considerable field-to-field variability in the number of wounded cells, suggesting marked heterogeneity and a focal nature of the injury. Mean SDs in cell injury index across 10 random images within a specimen were 0.06 in group I, 0.08 in group II, 0.15 in group III, and 0.32 in group IV.

TABLE 1. WEIGHT, AIRWAY PRESSURE, AND PULMONARY ARTERY PRESSURE AT BASELINE, BEGINNING, AND END OF EXPERIMENTAL VENTILATION; CHANGE IN DYNAMIC COMPLIANCE AND LUNG WEIGHT GAIN*

	6 ml/kg PEEP 3 (n = 6)	30 ml/kg PEEP 3 (n = 6)	40 ml/kg PEEP 3 (n = 7)	40 ml/kg ZEEP (n = 6)	p Value
Baseline					
Weight, kg	0.36 ± 0.03	0.33 ± 0.02	0.34 ± 0.02	0.33 ± 0.02	0.29
Paw, cm H ₂ O	12.38 ± 3.1	10.50 ± 1.72	12.32 ± 1.16	10.57 ± 2.1	0.26
PAP, cm H ₂ O	11.98 ± 4.2	10.12 ± 2.10	11.40 ± 4.18	8.71 ± 1.35	0.32
1 min					
Paw, cm H ₂ O	12.4 ± 3.1	33.1 ± 3.4	47.1 ± 4.2	38.2 ± 3.9	< 0.01
PAP, cm H ₂ O	13.5 ± 6.9	9.5 ± 2.5	12.6 ± 5.6	8.7 ± 2.3	0.25
30 min					
Paw (cm H ₂ O)	14.08 ± 2.8 [§]	37.2 ± 4.0 [§]	53.6 ± 6.0 [§]	51.0 ± 7.1 [§]	< 0.01
PAP (cm H ₂ O)	17.1 ± 14.6	9.37 ± 1.8	15.4 ± 6.7 [§]	14.7 ± 4.6 [§]	0.16 [¶]
%Δ Cdyn [†]	-4 ± 10.5	-8.9 ± 8.4	-73.3 ± 11	-76.8 ± 10	< 0.01
Lung weight gain, g [‡]	1.04 ± 0.15	1.36 ± 0.39	4.89 ± 1.48	5.22 ± 0.58	< 0.01

Definition of abbreviations: %Δ Cdyn = change in dynamic compliance; PAP = mean pulmonary artery pressure; PAW = peak airway pressure; PEEP = positive end-expiratory pressure; ZEEP = zero end-expiratory pressure.

* Data are expressed as mean ± SD.

† Because of the different volume histories, lung compliance comparisons were done between the relative (e.g., percentage change from the start) rather than absolute value.

‡ End lung weight - predicted lung weight.

§ p < 0.05, 30 minutes compared with 1 minute, paired t test.

|| One-way analysis of variance.

¶ Kruskal-Wallis test.

Cell Injury Index Correlated with Conventional Injury Parameters

The initial weight, pulmonary artery pressures, and airway pressures were similar in the four groups (Table 1). In groups III and IV, peak airway pressure, pulmonary artery pressure, and measures of edema (fall in inflation compliance and weight gain) all increased over the course of the experiment (Table 1).

Two representative light microscopic images contrast the normal architecture of a lung that was ventilated at group I settings with that of a lung from group IV (Figure 2, top). Note the diffuse alveolar damage, the widespread hyaline membrane formation, the perivascular hemorrhage, and the small airway epithelial injury in the group IV lung. The mean histologic injury score was 0.5 ± 0.5 in group II and increased to 7.0 ± 2.2 and 8.5 ± 0.6 in groups III and IV, respectively (Figure 2, bottom). The

difference in histologic injury score between groups III and IV was not statistically significant. Epithelial necrosis and cell sloughing were observed in distal airways and alveolar ducts. In lungs with the most severe injury, epithelial lesions also involved larger airways. There was no difference in the distribution of injury between subpleural and central lung regions.

The degree of cellular injury in subpleural alveoli, as reflected in the number of wounded cells per alveolus, correlated with traditional injury markers across the four experimental groups (Table 1 and Figure 3). There was no correlation between cell injury index and conventional injury parameters within groups, however. Furthermore, although the cell injury index of group IV was significantly greater than that of group III, none of the conventional injury markers distinguished between these two groups; that is, they failed to reveal a PEEP effect (Figure 3).

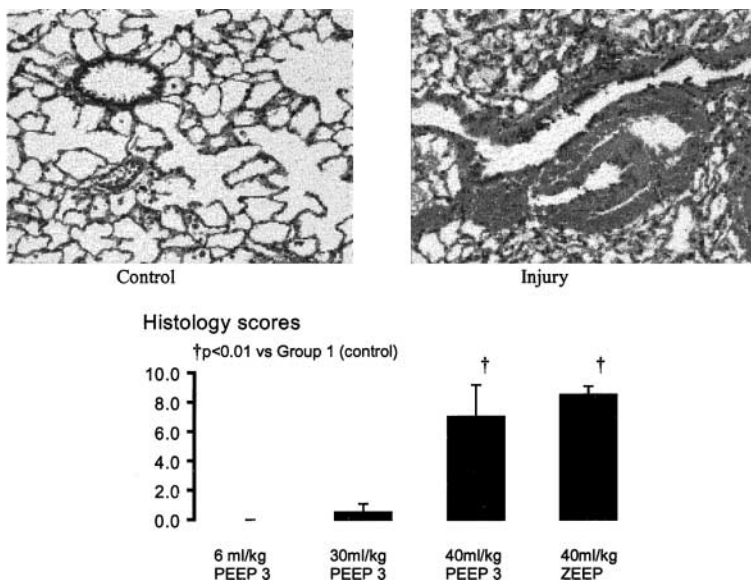


Figure 2. (Top) Representative histology images. (Left) Control (6 ml/kg PEEP) with normal lung architecture. (Right) Injurious ventilation (40 ml/kg ZEEP). Note hyaline membrane formation, perivascular hemorrhage and small airway epithelial injury. (Bottom) Semiquantitative histology scores based on the presence and the amount of hyaline membranes, perivascular hemorrhage, and small airway epithelial injury.

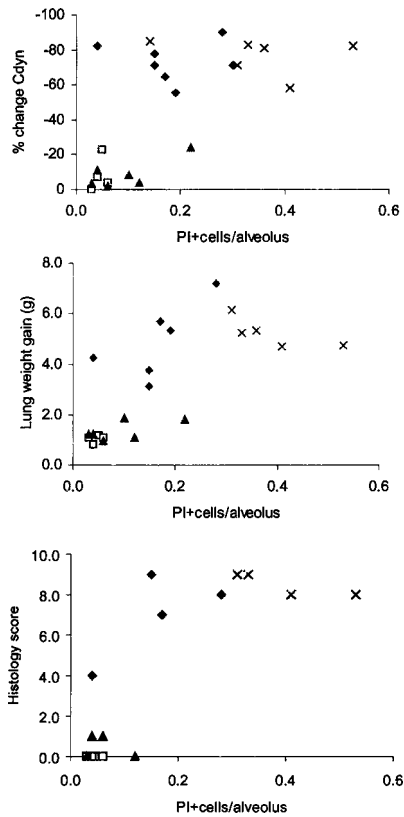


Figure 3. Correlation between the cell injury index and conventional injury markers across the four experimental groups. (Top) Change in dynamic compliance. (Middle) Lung weight gain. (Bottom) Histology score. Open squares, 6 ml/kg PEEP 3; closed triangle, 30 ml/kg PEEP 3; closed diamond, 40 ml/kg PEEP 3; ×, 40 ml/kg ZEEP; Cdyn = dynamic compliance.

Most Injured Cells Reseal upon Removal of the Injurious Stress

Injured lungs that were PI labeled after resumption of a noninjurious ventilator setting had a significantly lower cell injury index than lungs that were PI labeled during injurious mechanical ventilation (Figure 4). Specifically, the cell injury index fell from 0.25 ± 0.09 to 0.08 ± 0.08 after the injury stimulus had been removed ($p < 0.01$). In contrast, there was no significant effect of label application timing on conventional injury markers such

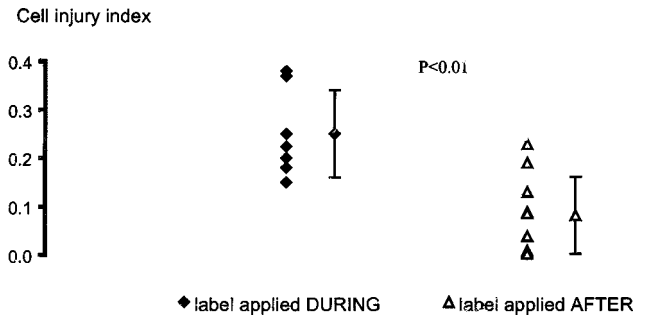


Figure 4. Average number of PI-positive cells per alveolus when the label was applied for 5 minutes either during or after the experimental ventilation. Both groups were ventilated for 30 minutes with V_T 40 ml/kg and ZEEP.

as change in airway and vascular pressures, weight gain, fall in inflation compliance, and histologic injury score (Table 2).

To test whether the lower cell injury index of postinjury labeled lungs could be explained by a normalization of vascular leakiness and the consequent exclusion of PI from the alveolar spaces, we harvested edema fluid from post injury labeled lungs and applied it to wounded A549 cells. PI staining of cells at the wound edge could be consistently demonstrated (data not shown). Therefore, we interpret the decrease in the number of PI-positive cells after resumption of noninjurious ventilation as evidence of restored plasma membrane integrity (i.e., wound resealing).

In Vitro Validation of a Method to Characterize Cell Injury and Resealing

Figure 5 shows three representative images of fluorescently labeled wounded cells in culture. In the left image (series 1), cells were wounded in the presence of FDx (green fluorescence). PI was added 1 minute later. Because resealing of the plasma membrane traps FDx inside the cytoplasm and prevents subsequent PI entry, the two labels do not colocalize. If the cell fails to reseal, FDx washes out, and PI gains entry and labels the nucleus. Based on the dual labeling method of series 1, we estimate a resealing rate of $79 \pm 10\%$ in this A549 cell-based wounding model. Estimates of resealing rates using the approach taken in the whole lung experiment (series 2 and 3) yielded very similar results ($87 \pm 20\%$, $p = 0.37$).

TABLE 2. CELL INJURY INDEX AND CONVENTIONAL INJURY MARKERS WITH THE LABEL (PROPIDIUM IODIDE) PERFUSED EITHER DURING OR AFTER EXPERIMENTAL VENTILATION

	40 ml/kg ZEEP with Label Perfused for 5 Minutes during the Injury (n = 7)	40 ml/kg ZEEP with Label Perfused for 5 Minutes after the Injury (n = 10)	p Value
Animal weight, kg	0.33 ± 0.03	0.32 ± 0.04	0.63
PAW start, cm H ₂ O	37.3 ± 3.4	37.9 ± 4.2	0.77
PAP start, cm H ₂ O	11.5 ± 2.2	11.7 ± 2.3	0.9
PAW end, cm H ₂ O	49.9 ± 6.7	49.6 ± 5.7	0.9
PAP end, cm H ₂ O	14.3 ± 2.8	17.4 ± 5.4	0.14
LIP, cm H ₂ O	25.7 ± 4.6	24.5 ± 3.2	0.55
%Δ Cdyn	-83.9 ± 8.5	-79.7 ± 9.8	0.21
Lung weight gain, g	4.9 ± 1.06	5.6 ± 0.6	0.18
Cell injury index	0.25 ± 0.09	0.08 ± 0.08	0.002

Definition of abbreviations: LIP = pressure at the lower inflection point of the inspiratory pressure–volume curve; PAP = mean pulmonary artery pressure; PAW = peak airway pressure; %Δ Cdyn = percent change in dynamic compliance; ZEEP = zero end-expiratory pressure.

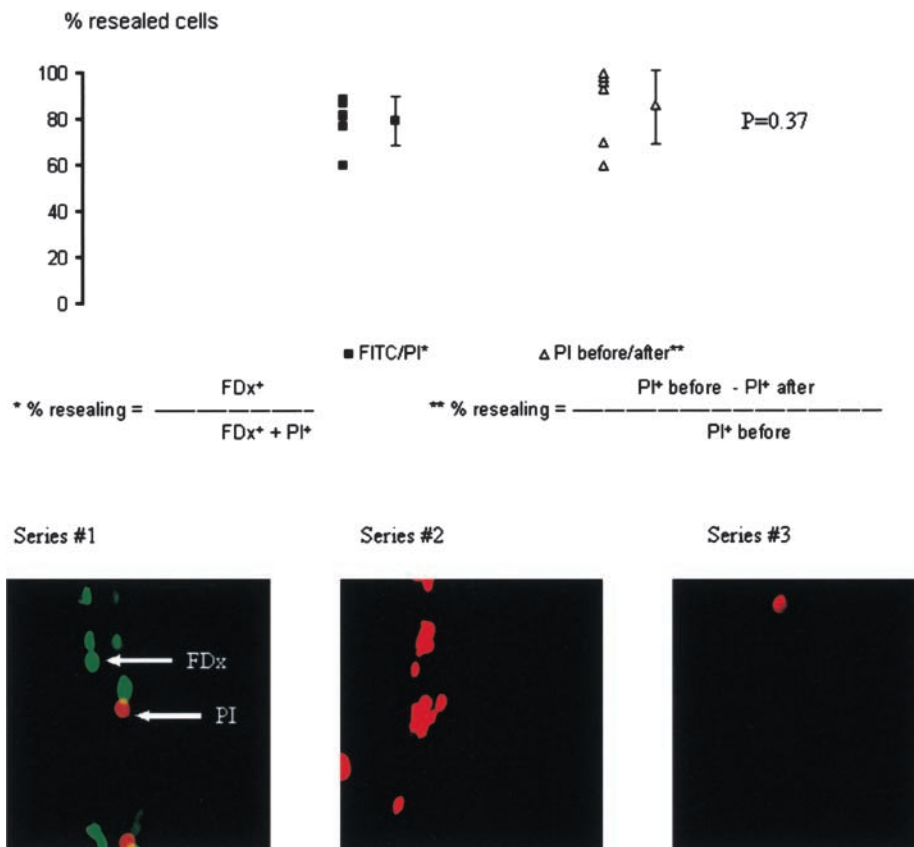


Figure 5. (Top) Comparison of two labeling methods for the assessment of cell resealing in a cell culture after scratch injury. Cell membrane repair was expressed as percentage of resealed cells from the total number of injured cells. (Bottom) Series 1: A459 cells after scratch injury in the presence of fluorescein-5-isothiocyanate labeled Dextran (FDx) followed by PI; series 2: A459 cells labeled with PI during the scratch injury; series 3: A459 cells with no label applied during the scratch injury. All three groups were incubated with PI after the scratch injury.

DISCUSSION

We have introduced a new method for quantifying cell wounding in an *ex vivo* rat model of VILI. The method identifies cells with either transient or permanent plasma membrane stress failure. We have validated the method by demonstrating the expected dependence of cell injury on VT and by correlating our index of cell wounding with conventional lung injury parameters. We have also shown that removal of injurious stress causes a decrease in the number of labeled cells and have attributed the decrease in labeling to a restoration of plasma membrane integrity, that is, wound resealing.

Our objective was to show that cells of ventilator-injured lungs undergo reversible plasma membrane stress failure; it was not to establish efficacy of a specific ventilation strategy in a clinically relevant disease model. Therefore, we chose an experimental approach that could be easily referenced and the results compared with data in the published literature (26, 27). Not surprisingly, the choice of VT was a major determinant of injury by any measure (Table 1 and Figures 1 and 2).

That alveolar epithelial and endothelial cells are targets of mechanical injury has been appreciated for decades (1–5). Whereas cells themselves are probably not the principle stress-bearing elements of the blood-gas barrier, they undoubtedly sense and transduce deforming stress. We know from *in vitro* studies of epithelial monolayers that relatively large strains must be applied to the substratum before a significant amount of wounding can be demonstrated (11, 14). A loss of barrier function and a change in the distribution of surface forces undoubtedly promote such conditions in the injured lung.

Because there is considerable topographical heterogeneity in both character and extent of mechanical ventilation associated lung lesions, electron microscopy is not a technique with which

one can easily quantify injury of an entire lung. In contrast, the PI labeling method gives information on a scale conducive to estimating whole lung injury. However, the method does not distinguish between epithelial, endothelial, and basement membrane lesions, all of which are subject to ventilator-induced stress failure. The relative determinants and susceptibilities of these structures to stress failure remain incompletely understood. There is a complex interplay between capillary pressure and flow, surface tension, lung volume, and the rate of lung expansion on the stress distribution along the blood-gas barrier. It is not known whether these variables interact with sufficient degrees of freedom to produce distinct disease specific patterns of cellular injury. Our light microscopic observations confirm earlier reports that VILI is associated with lesions in small airways and alveolar ducts (26, 28–30). Some of these structures may not be visible with single photon confocal microscopy because it is hard to illuminate tissue more than 50 μm below the pleural surface. Nevertheless, there was good agreement between the PI labeling-based injury index and the histologic injury score.

Given our choice of ventilator settings, it should come as no surprise that lungs in groups III and IV revealed distinctly more injury than lungs in groups I and II. Because of this bifurcation in group responses, there was a good correlation between the PI labeling-derived cell injury index and conventional measures of lung injury. There is no single gold standard of injury. Edema, hemorrhage, influx of inflammatory cells, cytokine levels, and gene expression of proteins as well as the number of cells with ultrastructural lesions reflect different dimensions of injury. They ought to be correlated, but there is no reason to believe that indices with different temporal expression profiles will be perfectly correlated at any one instant in time. Nevertheless, the statistically significant differences in cell injury estimates between

lungs of groups III and IV deserve closer scrutiny. It appears that the addition of a modest amount of PEEP (3 cm H₂O to group III) prevents cellular stress failure even though weight gain, mechanical impedance, vascular resistance, and light microscopic injury scores were similar between the two groups. The heterogeneous nature of the injury and spatial differences in sampling (the conventional markers were measured in the whole lung while the PI uptake was restricted to subpleural alveoli) may have contributed to the observed differences. Another possible explanation for the discordance between the PI labeling-based cell injury estimates and conventional lung injury parameters is to consider the PEEP effect real and the conventional injury parameters too insensitive to reveal it. PEEP is thought to protect the lungs from mechanical injury by minimizing the shear stress associated with the repeated opening and collapse of small airways and alveolar ducts (26, 31–33). This is particularly relevant in a preparation in which the transmural pressure is allowed to fall to zero on every breath. Recently, this mechanism of PEEP derived benefit has been challenged in favor of one that views the displacement of edema from small airways and alveoli to interstitial spaces as the key event (34). Nevertheless, the net effect of either mechanism could be a reduced local wall stress resulting in fewer injured cells (35). It must also be emphasized that inflation compliance and lung weight gain are not nearly as sensitive parameters of vascular permeability as is the filtration coefficient, which we did not measure (36). The latter might well have uncovered beneficial PEEP effects on edema formation in lungs ventilated with high tidal volumes. Finally, one should not assume that cell injury and vascular leakiness are always neatly correlated. A great deal of new information on the role of endothelial cell mechanics and cytoskeletal remodeling in the regulation of vascular permeability has emerged in recent years (37). Plasma membrane stress failure is but one of many stimuli that trigger cell remodeling and thereby mediate changes in fluid flux across the vascular wall (36).

We have attributed the difference in labeling between lungs that were perfused with PI during injury and lungs that were perfused with PI after injury to a wound healing response. Before discussing the biologic implications of this finding, we consider alternative interpretations and potential technical limitations of our methods.

First, we need to consider alternative mechanisms of PI uptake, such as fluid phase pinocytosis or simple diffusion. PI is a membrane impermeant nuclear label that is routinely used in cell viability assays. An extensive literature search failed to uncover specific documentation of PI uptake by pinocytosis. We consider this mode of entry unlikely based on the following observations: (1) There is virtually no PI uptake in cultured alveolar epithelial cells incubated for 30 minutes with PI in the presence of phorbol ester (as an endocytosis stimulator) unless cells are permeabilized (see Figure E1 in the online supplement). (2) Minimal uptake is observed when PI is administered for 30 minutes at non-injurious ventilator settings (see Figure 1 and Figure E2 of online supplement).

One of the central assumptions of the technique is that the local label concentration is high enough for PI to enter the cell and label its nucleus should a plasma membrane break occur. Because we perfused the lungs with PI containing solutions, this assumption is likely satisfied for endothelial cells. However, one cannot *a priori* assume that a sufficient amount of PI gains access to the alveolar space under conditions during which the filtration coefficient is relatively normal. In other words, vascular permeability could be a confounding variable and explain why fewer lung cells took up PI in experiments in which label perfusion was restricted to the post injury period. Two observations argue strongly against this interpretation. In several instances, we

sought to remove label from the vascular space by perfusing the preparation for 5 minutes with label free Krebs solution. We then cut the lung in 50- μ m thick coronal slices because we wanted to analyze the distribution of PI-positive cells with respect to small airways and alveolar ducts. These attempts invariably failed because virtually every cell in the specimen appeared labeled. We attributed this observation to our inability to remove label from alveolar edema fluid combined with the cell injury caused by cutting the specimen. In additional experiments, we removed edema fluid from lungs that had been label perfused after injury. The edema fluid was then applied to a monolayer of A549 cells, the monolayer wounded with a scalpel and subsequently imaged for PI fluorescence. Invariably, the cells near the wound edge were PI positive. Therefore, we conclude that even after removal of the injurious insult, sufficient amounts of PI enter the alveolar spaces to label injured pneumocytes.

Several lines of evidence suggest that removal of mechanical stress causes a rapid restoration of endothelial structure and vascular barrier function. In a series of experiments on isolated mesenteric frog vessels, Neal and Michel showed that increasing perfusion pressure opens both intraendothelial and interendothelial gaps and that these gaps recover within minutes of lowering pressure (38–40). The groups led by West and Mathieu-Costello and Dreyfuss and colleagues came to a similar conclusion after a detailed electron microscopic examination of ventilation and perfusion-injured lungs (1, 2, 41, 42). Neal and Michel argued that gap formation was an adaptive cellular stress response rather than the consequence of a basement membrane break (43). To our knowledge, we provide the first direct evidence that the VILI lesion is associated with transient loss of plasma membrane integrity. However, we do not know whether reversible plasma membrane stress failure is a necessary stimulus for strain-related remodeling of the blood-gas barrier.

In summary, we have demonstrated that ventilation-induced lung injury is associated with both reversible and irreversible forms of plasma membrane stress failure. The consequences of these events on lung inflammation and repair are of obvious clinical and biologic interest. Because the determinants of plasma membrane stress failure may not be intimately linked to the molecular mechanisms that govern membrane repair, lipid trafficking and membrane resealing should also be considered targets in the search for effective pharmacoprotection from VILI.

References

- Dreyfuss D, Basset G, Soler P, Saumon G. Intermittent positive-pressure hyperventilation with high inflation pressures produces pulmonary microvascular injury in rats. *Am Rev Respir Dis* 1985;132:880–884.
- Fu Z, Costello ML, Tsukimoto K, Prediletto R, Elliott AR, Mathieu-Costello O, West JB. High lung volumes increases stress failure in pulmonary capillaries. *J Appl Physiol* 1992;73:123–133.
- Costello ML, Mathieu-Costello O, West JB. Stress failure of alveolar epithelial cells studied by scanning electron microscopy. *Am Rev Respir Dis* 1992;145:1446–1455.
- Bachofen H, Schurch S, Weibel ER. Experimental hydrostatic pulmonary edema in rabbit lungs: barrier lesions. *Am Rev Respir Dis* 1993;147:997–1004.
- John E, McDevitt M, Wilborn W, Cassidy G. Ultrastructure of the lung after ventilation. *Br J Exp Pathol* 1982;63:401–407.
- Dreyfuss D, Saumon G. Ventilator-induced lung injury: lessons from experimental studies. *Am J Respir Crit Care Med* 1998;157:294–323.
- Dos Santos CC, Slutsky AS. Mechanisms of ventilator-induced lung injury: a perspective (invited review). *J Appl Physiol* 2000;89:1645–1655.
- Parker JC, Hernandez LA, Peevy KJ. Mechanisms of ventilator-induced lung injury. *Crit Care Med* 1993;21:131–143.
- Gajic O, Lee J-H, Doerr CH, Hubmayr RD. Assessment of ventilator-induced plasma membrane wounding and repair in the intact lung [abstract]. *Am J Respir Crit Care Med* 2002;165:A783.
- Vlahakis NE, Schroeder MA, Pagano RE, Hubmayr RD. Role of defor-

- mation-induced lipid trafficking in the prevention of plasma membrane stress failure. *Am J Respir Crit Care Med* 2002;166:1282–1289.
11. Vlahakis NE, Hubmayr RD. Plasma membrane stress failure in alveolar epithelial cells (invited mini review). *J Appl Physiol* 2000;89:2490–2496.
 12. West JB, Mathieu-Costello O. Structure, strength, failure, and remodeling of the pulmonary blood-gas barrier. *Annu Rev Physiol* 1999;61:543–572.
 13. Stroetz RW, Vlahakis NE, Walters BJ, Schroeder MA, Hubmayr RD. Validation of a new live cell strain system: characterization of plasma membrane stress failure. *J Appl Physiol* 2001;90:2361–2370.
 14. Tschumperlin DJ, Oswari J, Margulies AS. Deformation-induced injury of alveolar epithelial cells: effect of frequency, duration, and amplitude. *Am J Respir Crit Care Med* 2000;162(2 Pt 1):357–62.
 15. McNeil PL, Terasaki M. Coping with the inevitable: how cells repair a torn surface membrane. *Nat Cell Biol* 2001;3:E124–E129.
 16. Terasaki M, Miyake K, McNeil PL. Large plasma membrane disruptions are rapidly resealed by Ca²⁺-dependent vesicle-vesicle fusion events. *J Cell Biol* 1997;139:63–74.
 17. Steinhardt RA, Bi G, Alderton JM. Cell membrane resealing by a vesicular mechanism similar to neurotransmitter release. *Science* 1994;263:390–393.
 18. Grembowicz KP, Strague D, McNeil PL. Temporary disruption of the plasma membrane is required for c-fos expression in response to mechanical stress. *Mol Biol Cell* 1999;10:1247–1257.
 19. Liu M, Tanswell AK, Post M. Mechanical force-induced signal transduction in lung cells. *Am J Physiol* 1999;277:L667–L683.
 20. Wirtz HR, Dobbs LG. The effects of mechanical forces on lung functions. *Respir Physiol* 2000;119:1–17.
 21. Parker JC, Ivey CL, Tucker JA. Gadolinium prevents high airway pressure-induced permeability increases in isolated rat lungs. *J Appl Physiol* 1998;84:1113–1118.
 22. Uhlig S. Mechanotransduction in the lung: ventilation-induced lung injury and mechanotransduction: stretching it too far? *Am J Physiol Lung Cell Mol Physiol* 2002;282:L892–L896.
 23. McNeil PL, Ito S. Gastrointestinal cell plasma membrane wounding and resealing *in vivo*. *Gastroenterology* 1989;96:1238–1248.
 24. Lin YC, Ho CH, Grinnell F. Fibroblasts contracting collagen matrices form transient plasma membrane passages through which the cells take up fluorescein isothiocyanate-dextran and Ca²⁺. *Mol Biol Cell* 1997;8:59–71.
 25. Broccard AF, Hotchkiss JR, Vannay C, Markert M, Sauty A, Feihl F, Schaller MD. Protective effects of hypercapnic acidosis on ventilator-induced lung injury. *Am J Respir Crit Care Med* 2001;164:802–806.
 26. Muscedere JG, Mullen JB, Gan K, Slutsky AS. Tidal ventilation at low airway pressures can augment lung injury. *Am J Respir Crit Care Med* 1994;149:1327–1334.
 27. Tremblay L, Valenza F, Ribeiro SP, Li J, Slutsky AS. Injurious ventilatory strategies increase cytokines and c-fos mRNA expression in an isolated rat lung model. *J Clin Invest* 1997;99:944–952.
 28. Marini JJ. Ventilator-induced airway dysfunction? *Am J Respir Crit Care Med* 2001;163:806–807.
 29. Goldstein I, Bughalo MT, Marquette CH, Lenaour G, Lu Q, Rouby JJ. Mechanical ventilation-induced air-space enlargement during experimental pneumonia in piglets. *Am J Respir Crit Care Med* 2001;163:958–964.
 30. D'Angelo E, Pecchiari M, Baraggia P, Saetta M, Balestro E, Milic-Emili J. Low-volume ventilation causes peripheral airway injury and increased airway resistance in normal rabbits. *J Appl Physiol* 2002;92:949–956.
 31. Gattinoni L, D'Andrea L, Pelosi P, Vitale G, Pesenti A, Fumagalli R. Regional effects and mechanism of positive end-expiratory pressure in early adult respiratory distress syndrome. *JAMA* 1993;269:2122–2127.
 32. Lachmann B. Open up the lung and keep the lung open. *Intensive Care Med* 1992;18:319–321.
 33. Argiras EP, Blakeley CR, Dunnhill MS, Otramski S, Sykes MK. High PEEP decreases hyaline membrane formation in surfactant deficient lungs. *Br J Anaesth* 1987;59:1278–1285.
 34. Hubmayr RD. Perspective on lung injury and recruitment: A skeptical look at the opening and collapse story. *Am J Respir Crit Care Med* 2002;165:1647–1653.
 35. Bilek AM, Dee KC, Gaver DP. Lung epithelial cell injury in an *in vitro* model of airway reopening [abstract]. *FASEB J* 2002;16:A409.
 36. Michel CC, Curry FE. Microvascular permeability. *Physiol Rev* 1999;79:703–761.
 37. Dudek SM, Garcia JG. Cytoskeletal regulation of pulmonary vascular permeability. *J Appl Physiol* 2001;91:1487–1500.
 38. Neal CR, Michel CC. Transcellular openings through microvascular walls in acutely inflamed frog mesentery. *Exp Physiol* 1992;77:917–920.
 39. Neal CR, Michel CC. Transcellular openings through frog microvascular endothelium. *Exp Physiol* 1997;82:419–422.
 40. Neal CR, Michel CC. Openings in frog microvascular endothelium induced by high intravascular pressures. *J Appl Physiol* 1996;492:39–52.
 41. Elliott AR, Fu Z, Tsukimoto K, Prediletto R, Mathieu-Costello O, West JB. Short-term reversibility of ultrastructural changes in pulmonary capillaries caused by stress failure. *J Appl Physiol* 1992;73:1150–1158.
 42. Dreyfuss D, Soler P, Saumon G. Spontaneous resolution of pulmonary edema caused by short periods of cyclic overinflation. *J Appl Physiol* 1992;72:2081–2089.
 43. Savla U, Neal CR, Michel CC. Openings in frog microvascular endothelium at different rates of increase in pressure and at different temperatures. *J Physiol (Lond)* 2002;539:285–293.